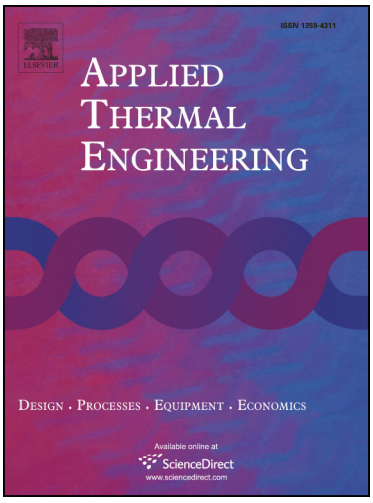
Journal Pre-proofs



A Comprehensive Approach to Analyze the Discrepancies in Heat Transfer Characteristics Pertaining to Radiant Ceiling Heating System

Yakup Karakoyun, Ozgen Acikgoz, Alican Çebi, Aliihsan Koca, Gürsel Çetin, Ahmet Selim Dalkilic, Somchai Wongwises

PII: S1359-4311(20)33991-0
DOI: https://doi.org/10.1016/j.applthermaleng.2020.116517
Reference: ATE 116517

To appear in: *Applied Thermal Engineering*

Received Date: 31 August 2020
Revised Date: 20 December 2020
Accepted Date: 23 December 2020

Please cite this article as: Y. Karakoyun, O. Acikgoz, A. Çebi, A. Koca, G. Çetin, A. Selim Dalkilic, S. Wongwises, A Comprehensive Approach to Analyze the Discrepancies in Heat Transfer Characteristics Pertaining to Radiant Ceiling Heating System, *Applied Thermal Engineering* (2020), doi: https://doi.org/10.1016/j.applthermaleng.2020.116517

This is a PDF file of an article that has undergone enhancements after acceptance, such as the addition of a cover page and metadata, and formatting for readability, but it is not yet the definitive version of record. This version will undergo additional copyediting, typesetting and review before it is published in its final form, but we are providing this version to give early visibility of the article. Please note that, during the production process, errors may be discovered which could affect the content, and all legal disclaimers that apply to the journal pertain.

© 2020 Published by Elsevier Ltd.

A Comprehensive Approach to Analyze the Discrepancies in Heat Transfer Characteristics Pertaining to Radiant Ceiling Heating System

Yakup Karakoyun[a], Ozgen Acikgoz[b]*, Alican Çebi[b], Aliihsan Koca[c], Gürsel Çetin[d], Ahmet Selim Dalkilic[b], Somchai Wongwises[e,f]

[a]Energy Division, Department of Mechanical Engineering, Hakkari University, Hakkari, 30000, Turkey

[b]Heat and Thermodynamics Division, Department of Mechanical Engineering, Yildiz Technical University, Istanbul 34349, Turkey

[c]Fatih Sultan Mehmet Vakif University, Faculty of Engineering, Istanbul, 34445, Turkey

[d]Mir Arastirma ve Gelistirme A.S., 34220 Istanbul, Turkey

[e] Department of Mechanical Engineering, Faculty of Engineering, King Mongkut's University of Technology Thonburi (KMUTT), Bangkok 10140, Thailand

[f]National Science and Technology Development Agency (NSTDA), Pathum Thani 12120, Thailand

Highlights

- Heated radiant ceiling, a rarely studied system, is examined.
- A novel model based on CFD, ANN, and experimental data is developed.
- Predictability of ANN method is found to be within ±15% deviation range.
- New heat transfer coefficients are proposed for radiant heated ceiling.

Abstract

Radiant heating/cooling systems are being popular thanks to their ability of regulating the living-environment with the use of low temperature heating and high temperature cooling. In this work, an artificial neural network investigation is carried out to predict heat transfer characteristics over a heated radiant ceiling. Experimental tests consisting of 28 case studies, obtained through varying supply water temperature, are conducted. A computational method, including the Boussinesq approach using k-ε RNG model, is also employed to increase the number of case studies in order to use them in artificial neural networks investigation that applies Levenberg-Marquardt training function. Thus, total data number have been increased from 28 to 74 by a simulation software. Estimations of artificial neural networks method are compared with experimental data, and seen that the outputs are compatible with each other, where most of deviations are within the range of ±15%. According to this result, experimental data can be increased by a numerical simulation software and evaluated by one of the artificial intelligence techniques, successfully. In conclusion, the heat transfer coefficients to use in the radiant ceiling heating applications are proposed

as 0.9 W/m^{2}K, 5.3 W/m^{2}K, and 7.0 W/m^{2}K for convective, radiative, and total heat transfer coefficients, respectively.

Keywords: Heat transfer coefficients, Thermal output, Radiant ceiling heating; ANN; CFD

*Corresponding author.
Tel.: +90 212 3832821; fax: +90 212 3832914; E-mail address: oacikgoz@yildiz.edu.tr (O. Acikgoz).

On behalf of all authors, the corresponding author states that there is no conflict of interest.

1. Introduction

Low temperature heating and high temperature cooling applications are being utilized commonly due to their energy saving potential. The radiant heating and cooling systems may be identified as one the aforementioned systems. Along with the low exergy destruction characteristics of such systems, the radiant heating/cooling systems may enable more relaxed living-environment by diminishing free convection heat transfer associated with natural convection currents compared to conventional domestic radiators or fan-coils -that is a major reason for discomfort in living environments- as well as growing radiative heat transfer by conditioning the wide surfaces as heat sources/sinks with desired and relatively lower/higher temperatures, respectively. According to a study conducted by Mancini et al. [1], 41.7 % of consumed energy is expended to meet domestic purposes. In the light of this information, if any enhancement related to increasing the performance of radiant heating/cooling system has been achieved, this will eventually result in decreasing energy consumption in buildings.

The heat transfer characteristics in constructions has had a significant impact on the loads determined by building energy numerical software, thermal comfort, and energy economics. It is quite obvious that radiative and convective phenomena that correspond to radiative and convective heat transfer coefficients account for utmost results within the calculation and dimensioning path of radiant heating and cooling systems. In addition, as figured out by some researchers in the field [2-6], the most operative factor in the dimensioning process and thermal comfort assessments of radiant systems is the convective heat transfer coefficient.

In the literature, one can meet with a great number of investigations over heating and cooling systems in living places with their surrounding surfaces. What is more, among various researches on radiant systems, a remarkable number of studies are observed about floor, wall heating, and cooling preferences. On the other hand, though not examined as much as the above mentioned ones, cooling through ceiling is also one dealt with issue. Nonetheless, in this context, condensation over surfaces has still been the foremost disadvantage of this cooling technique. Though it is being utilized in substantial extent of applications, heating from ceiling is possibly the least area on which researchers have been involved in. The studies

concerning the thermal performance and heat transfer characteristics of radiant heated ceilings are summarized as follows.

The applicability of the radiant heated ceilings with considering the energy consumption and thermal performance was being subjected to some experimental and numerical studies. Liu and Lin [7] compared various residential building heating systems including ceiling heating by means of their energy and exergy performances. Based on the conducted numerical study the stratum ventilation showed the best energetic and exergetic performance among the all studied heating systems. According to the presented results, while wall radiator heating system showed the worst exergetic performance, the radiant heated floor and ceiling showed better performances. If radiant heated floor and ceiling are compared via exergy consumption, the ceiling results are lower than the floor results. It is concluded that the amount of exergy consumption of radiant heated floor and ceiling is strictly depending on the surface coverage materials. Lateb and Fellouah [8] conducted a theoretical study to analyse the radiant heated ceiling system by considering the highly cold thermal environments. It is stated that radiant heated ceiling system is an efficient conditioning system with regarding the energy consumption. Bojić et al. [9] used a simulation program (EnergyPlus) to analyze the performance of the low temperature radiant heating systems (floor, wall, ceiling and floor-ceiling heating systems) in terms of energy, environment, and economics. In the study, the radiant floor-ceiling heating system showed the highest performance considering energy consumption, exergy consumption, CO2 emission, operating cost, and boiler power.

Zhao et al. [10] performed some experiments in a domestic construction in a province of China. One of the results of the study, they have pointed out that through reducing the supply water temperatures, energy saving of the system can be note worthily improved, although the supply water temperature is lower than 35^{o}C. Also, Safizadeh et al. [11] claimed that radiant ceiling heating is preferable due to the providing low temperature heating and giving the opportunity of renovating the buildings with demanding the less amount of changes. They numerically studied the performance of low temperature radiant ceiling heating system using computational fluids dynamics (CFD) and simulation tool TRNSYS. According to the study, using low temperature radiant ceiling heating system does not result in thermal asymmetry in contrast to the result of work done by Fanger et al. [12]. Via providing low thermal asymmetry, considered radiant heating system prevents the thermal sensation asymmetries between the different parts of human body. Authors also conducted an experimental study [13] to assess the applicability of the low temperature radiant ceiling heating system with regarding the thermal comfort in old structures. As a result of their experimental work, the considered system ensures the neutral thermal sensation at the lots part of the body.

Yuan et al. [14] stated that the thermal discomfort, high energy consumption, radiant asymmetry, etc. resulted from the lack of knowledge about the radiant ceiling heating/cooling systems' thermal

characteristics. Authors conducted an experimental-numerical study to develop a model that defines the thermal characteristics between surface temperature and total heat flux. It is claimed that the proposed model can be used in wide range of applications as operating, sizing and dimensioning, thermal comfort etc.

Miriel et al. [15] experimentally analyzed the thermal performance of a radiant ceiling heating/cooling system regarding the energy consumption and thermal comfort. A simulation model using TRNSYS was proposed which verified by the results of experiments. Another aim of the study is expressed as identifying the thermal limits of radiant ceiling heating and cooling systems. As a result of the study, it is stated that radiant ceiling systems can be applied to buildings with ensuring the proper thermal insulation. The utilized radiant heated ceiling system showed high performance when set-temperature of room is relatively low at night period.

From heat transfer insight, along with the deductions through the relevant literature survey, it is clear that while considering the designing, dimensioning, and thermal comfort of a living environment, the key point is defining the heat transfer characteristics of the system that are composed of heat transfer coefficients and heat fluxes.

Koca and Cetin [16] stated that the radiant ceiling surface may not be sufficient to provide thermal comfort in cold weather conditions. Thus they tried to integrate radiant wall systems to current ceiling system and then experimentally analyze the combined system. The heat transfer characteristics of the radiant heated ceiling, wall, and ceiling-wall system were evaluated. In order to analyze and discuss the heat fluxes and heat transfer coefficients of indicated systems a thermally well-controlled climatic test chamber was constructed. In conclusion, new correlations were proposed to determine the total, radiative, and convective heat fluxes of radiant heated ceiling and walls. Additionally, the total heat transfer coefficients for both system were determined and given as 8.57 W/m^2K and 7.28 W/m^2K for radiant heated wall and ceiling, respectively. It is indicated that the experimentally defined coefficients are higher than the proposed values in the current literature and standards. Thus, the authors concluded that the coefficient values which are given in the literature are under estimated.

Causone et al. [17] experimentally investigated the heat transfer characteristics of radiant heated/cooled ceiling of a room. While heated cylinders simulated the heat gains in test chamber, the cooled surfaces simulated the heat losses. Authors indicated that, the reference temperatures have important role in determination of heat transfer characteristics of such systems. According to the results of experimental study, the total, radiative, and convective heat transfer coefficients for radiant heated ceiling were measured as 5.8 W/m^2K, 5.6 W/m^2K, and 0.3 W/m^2K, respectively. It is underlined that the values of given coefficients are strictly depend on the reference temperatures.

Yuan et al. [18] proposed new correlations for determination of heat flux and heat transfer coefficients of a radiant heated/cooled ceiling system. The given correlations were derived from experiments that carried out in a climate chamber. It is expressed that taking account the supply water temperature and the operative temperature, differs the proposed correlation from other correlations in the literature. According the results of experimental studies, the radiative heat transfer coefficients in both heating and cooling modes showed the similar results as in the range of 5.2 – 5.5 W/m^2K. When considering the convective heat transfer coefficients, it is seen that the values are quite lower than the values of radiative heat transfer coefficients, which means that the dominant heat transfer mechanisms in the radiant heated/cooled ceiling is the radiation.

Cholewa et al. [19] experimentally analyzed a radiant heated/cooled ceiling system to define the heat transfer coefficients of such systems, properly. Authors indicated that using the surface heat emitters gives the more accurate results on this issue. According to the results of experimental study, it is stated that the heat transfer coefficients that given in open literature are over-estimated, particularly for radiant heated ceilings. Additionally, while 5.4 W/m^2K is proposed as new total heat transfer coefficient for the sitting person, 5.6 W/m^2K is for standing person in radiant heated ceiling. Due to the relatively low air motion it is claimed that the value of the convective heat transfer coefficient for same heating system is nearly zero.

With the evaluation of a low-energy structure constructed in the University of Tokyo as an investigational study, Li et al. [20] stated that there were no standard for the in situ performance valuation of radiant heating and cooling systems. From this point of forth, they have intended to put out their outcomes in order to show their knowledge and for their data to be a reference point for similar systems. It was determined that from water to room heat transfer coefficient was 3.7 W/m^2K and 4.8 W/m^2K in heating and cooling approaches, correspondingly.

It is indicated in the study done by Hu and Niu [21], even though there exists lots of experimental and numerical works related to determination of the heat transfer characteristics of radiant heating/cooling applications, the problems with the estimation of heating/cooling capacities are still continuing. The existence of such estimation problems may cause higher energy consumption and thermal discomfort. It can be stated that one of the reasons of these load estimation problems is led by the inappropriately determined heat transfer coefficients that characterize the thermal behavior of the system. Furthermore, in a study [22] that compares the heat transfer coefficients of radiant applications which are given in the open sources and related standards, it is shown that the proposed heat transfer coefficients are showing discrepancies, even for the similar thermal conditions. For instance, the total heat transfer coefficient for radiant heated ceiling varies in the range of 5.6 – 7.28 W/m^2K.

As the open literature investigated comprehensively, it can be clearly seen that the artificial neural networks or other artificial intelligence approaches have been commonly implemented in prediction of building

energy consumption, determination of heating/cooling loads, energy demands, performance analyses etc. For example, Zhang et al. [23] suggested a new optimization method to optimize the building energy consumption by utilizing various analysing approaches. The proposed optimization method consists of an artificial neural network (ANN), a genetic algorithm (GA), a fuzzy logic controller (FLC), and a multivariate regression analysis (MRA). Jihad and Tahiri [24] used the artificial neural networks to estimate the energy demand of buildings in a selected zone. The results of ANN approach showed 98.7% accuracy for the estimation. In order to estimate the cooling load precisely Yokohama et al. [25] recommended a method applying the neural networks. Additionally, the effects of the relative humidity and air temperature on cooling load also examined. Benedetti et al. [26] proposed novel approaches utilizing the artificial neural networks for the controlling the energy consumption of buildings. The given methods were also assessed by means of their precision. Pino-Mejías et al. [27] conducted a study on artificial neural networks and linear regression models to determine the energy consumption, energy demand and CO_2 emissions of an office. 8 fundamental design parameters were selected and 77.000 cases were studied. It is concluded that the utilized ANN model showed a sufficiently well performance. Olofsson and Andersson [28] proposed an artificial neural network model to predict the long term energy demand using the short term values. The suggested model was carried out on various buildings in domestic usage with acceptable deviations.

There exists limited amount of studies that concern the heat transfer characteristics of radiant heating/cooling systems using ANNs. It should be understood that there is no paper using ANN analyses on the investigated subject. The relevant studies are summarized as follows. Acikgoz et al. [29] experimentally studied the heat transfer characteristics of a real-sized room with various configurations of heated walls. In their study, several ANN approaches were applied to further identify the thermal characteristics of radiant heating system. As a result of work, they concluded that Levenberg-Margurdt network gave the most accurate results through several approaches. Additionally, average convective, radiative, and total heat transfer coefficients which are the main parameters of heat transfer characteristics were proposed as 2.7 W/m^2K, 5.0 W/m^2K, and 9.0 W/m^2K, respectively. Karadag and Akgobek [30] estimated the heat transfer coefficients pertaining to radiant floor heating system using artificial neural networks (ANN). The trained values were obtained from the open literature. According to the results of artificial neural network analysis, it is stated that the indicated estimation approach can be used in radiant systems in terms of convective heat transfer.

Given the reasons for properly determining the heat transfer characteristics of the radiant heating and cooling applications properly have been stated in the previous paragraphs, the key point of this present investigation is to enable comprehensive practical and numerical proof to better comprehend the heat transfer characteristics of the radiant heated ceiling surfaces, along with composing an ANN-based approach to ascertain best-fitting model. In the current study, at the beginning, using an experimental facility,

measurements have been conducted on a ceiling heating application and 28 case studies have been obtained. As well as aiming to increase the number of case studies and to provide a numerical approach to implement in such systems, a computational method have been employed. Furthermore, it should be seen that for the derived correlations to be capable of representing flow, as well as radiative heat transfer pattern through the radiant ceiling heating application, experimental and computational case studies are carried out within a wide boundary condition interval, while in the experimental study different supply water temperatures are also performed. In the last step of the investigation, a number of ANN models have been performed to obtain the most favorable ANN model with regard to determining heat flux values through a heated ceiling along with radiative, convective, and total heat transfer coefficients occurring over the examined surface. To the best of authors' knowledge, there is no paper in open sources related to radiant heating systems having the combination of CFD for extending operating range of experimental work and ANN for evaluation of obtained data from experimental data and ANN analyses with high accuracy as well as the vast majority of the HTC values between ±15% deviation bands.

2. Experimental Apparatus

2.1 Construction of the experimental chamber

To build a radiant heated radiant ceiling system (from this point forward HRC), which is capable of providing boundary conditions spanning a broad interval, a test chamber was established, and these values are presented in Table 1. Fig. 1a demonstrates that the experimental chamber is made up of four parts of ceiling (volume 4), floor (volume 3), façade (volume 2), and tested zone (volume 1). Radiant ceiling panels have been placed within the test zone of which ceiling area is 16 m^2 and internal height is 3 m, suggested also in EN 1264-5 [31] and BS EN 14037-1 [32]. Table 2 shows the total heat transfer coefficient values of the wall and ceiling components. It should be stated that thermal stability of the surroundings were ensured via mechanic air conditioners. The emissivity values of the surfaces within the chamber were calculated by means of thermocouples and a thermal imaging camera, and pertaining method to achieve this purpose was given in [33]. General requirements of the ANSI/ASHRAE Standard 138 [34] are carried out by the practical preparations and thermos-physical properties of the test setup. The key deviation from the ANSI/ASHRAE standard 138 [34] is that in the current experimental chamber, sided volumes equipped with air conditioning units provide suitable boundary circumstances, whereas, the relevant standard suggests that the room should be conditioned through a distinct conditioning equipment attached to inner surfaces. It should be noted that there is a chiller unit in Fig. 1, so ceiling cooling research is also possible by means of this setup that is not the subject of the current research.

2.2 Hydraulic circuit

In order to supply proper inlet water temperatures and flow rates which flow through the HRC panels, a hydraulic system was established for the test chamber. Fig. 1b gives the feature of the hydraulic line, and components found on this line can be summarized in the following sentences. The buffer tank in which water is kept by means of electric resistances, four way valve in which the supply water temperature is altered to the demanded value through combining the source and return fluids. Three way valve, in which the mass flow rate is reached to targeted value accurately. The ultrasonic flow meter measuring the mass flow rate and providing input for the data logger. Afterward, the prepared water reaches the manifold and thus HRC panels for activating the heat transfer.

Furthermore, three components comprise HRC panels produced for the current investigation and are as follows: gypsum board, heating pipe serpentine and thermal insulation material. The serpentine has been placed between gypsum board and insulation material. The gypsum board and isolation thicknesses are 15 mm and 20 mm, respectively. The serpentine is made up of polyethylene pipes having an external diameter of 10.1 mm and pipe spacing of 55 mm. Additionally, expanded polystyrene has been chosen as a back front insulation material, whose total heat transfer coefficient values is 0.039 W m^{-1} K^{-1}. The dimensions of the panels are 0.6 m x 1.2 m. The chamber is equipped with 12 panels that are attached over the ceiling.

2.3 Equipment procured for measurements

Utilizing a K-type thermocouple, that was stationed at the middle of the chamber; the indoor air temperature was measured. HRC surface temperature was measured via five surface temperature transducers (TS8-(1,5)) mounted over the surface of representative panel (Fig. 2). The average value of those temperatures was taken as the heated surface temperature (Ts). The thermal comfort measurement was positioned at the middle of the room, and placed to determine the operative temperature, as well. To determine the area-weighted unheated surface temperature, which is defined by ASHRAE Standard 55 [35], one surface temperature sensor was hanged at the center of all unheated surfaces. Since, the unheated surfaces are made from aluminum which is high-conductive; taking measurements only from the mid positions of the surfaces was evaluated adequate. It should also be seen that all temperature transducers were satisfactorily calibrated in an interval spanning between 30^{o}C and 50^{o}C. Uncertainty analyses regarding with the all cases have been given in authors' previous publication in detail [36].

Supply water flow rate has been obtained using an ultrasonic flow-meter of which uncertainty level is ±1%. The inlet and outlet temperatures belonging to HRC, which take place on the hydraulic line were measured (T_{w1} and T_{w2}). To follow and keep under control the water temperature flowing through pipes, temperature sensors were stationed in the buffer tank (T_{w3}), between the four-way valve and the pump, (T_{w4}), and at the inlet (T_{w6}) and outlet (T_{w5}) of the chiller.

2.4 Experimental solution procedure

The most trustable studies are ones depending on experimentations conducted in a real-size experimental chamber such as that of the above detailed room. The supply water mass flow rate and other significant conditions were kept constant at wished levels. In addition, the case studies were implemented according to the standard EN 14240 [37] at steady state conditions. To bring the inner surfaces of the chamber (volume-1) into a desired interval, the volumes have been adjusted at definite temperatures till the essential intervals are reached. It should be noted that steady-state conditions have been acquired after approximately 5-6 h, in terms of all variants influencing the solution of theoretical calculations. Additionally, before the start of a study, supply water was flowed in the HRC to keep the surfaces at required temperature, and the temperatures of unheated surfaces as well as the air temperature were altered subject to the heat output of the panels.

Throughout the tests, mass flow rate of the water ($\dot{m}_w$), supply (T_{w1}) and return water temperatures (T_{w2}) were recorded to determine the total heat fluxes by the HRC panels. The operative temperature which was found experimentally by means of the thermal comfort device, was utilized in the determination of total heat transfer coefficient. In order to ascertain the convective heat transfer coefficient, air temperature transducer (T_{a1}), stationed at the center of the enclosure, was employed. The heat losses from back fronts of the HRC panels were acquired through the temperature differences of measured back front temperatures of the ceiling panel (T_{p1}), outer surface temperature (T_{p4}) of the HRC structures, isolation width, surface area of the panel (A) and total heat transfer coefficient (U) of the ceiling zone.

Outcomes on mean values have been obtained within the time intervals of 30 min. in which steady conditions were enabled. Series of tests were realized through altering the HRC surface temperatures. As soon as the heated surface and indoor air temperatures reached steady state level at the interval of 0.1 K/min, tests were initiated. With regard to the measurements, total (h_t), radiant (h_r) and convective (h_c) heat transfer characteristics were assessed and the outputs were detailed in Section 6.

3. Theoretical Calculations

Total heat transfer rate by the panels (Q_t); radiative heat transfer to the unheated surfaces (Q_r), convective heat transfer to the air (Q_c) and conduction heat loss from the backside of the panels (Q_{loss}) are expressed in Eq. (1)

$$Q_t = Q_r + Q_c + Q_{loss} \tag{1}$$

Overall beneficial heat transfer rate by the radiant panel, was revealed in relation to heat-flux density ($\dot{q}_{tot}$) along the panel surface, and was formulated via the differences of the overall panel heat-flux density ($\dot{q}_{pan}$) and the heat loss density ($\dot{q}_{loss}$):

$$\dot{q}_t = \frac{\dot{m}_w cp \Delta T_w}{A} - \dot{q}_{loss} \tag{2}$$

where, $\dot{q}_t$ is obtained by the practical measurements of water temperature difference between the inlet ($T_{w,1}$) and the outlet ($T_{w,2}$) temperatures of panel, and supply water flow rate. Total heat-flux density from the radiant system arises as radiation and convection and stated as follows:

$$\dot{q}_t = \dot{q}_r + \dot{q}_c \tag{3}$$

In addition, the total heat-flux density that includes convection and radiation may be defined as follows:

$$F_{s-j} = \frac{1}{A_i} \int_{A_i} \int_{A_j} \frac{\cos\theta_i \cos\theta_j}{\pi R^2} dA_i dA_j \tag{4}$$

where, T_a (K) is air temperature, T_{AUST} (K) is the area weighted average unheated surface temperature, h_c (W m^{-2} K^{-1}) is the convective and h_r (W m^{-2} K^{-1}) is the radiative heat transfer coefficient.

To calculate the radiative heat transfer coefficient, average unheated surface temperature (T_{AUST}) was employed as the reference temperature that was acquired by means of the view factors.

$$T_{AUST} = \sqrt[4]{\sum_{j=1}^{n} \left(F_{s-j} \; T_j^4 \right)} \tag{5}$$

$$F_{\varepsilon_{s-j}} = \frac{1}{\left[\left(1-\varepsilon_s\right)/\varepsilon_s \right] + \left(1/F_{s-j}\right) + \left(A_s/A_j\right)\left[\left(1-\varepsilon_j\right)/\varepsilon_j \right]} \tag{6}$$

$$F_{s-j} = \frac{1}{A_i} \int_{A_i} \int_{A_j} \frac{\cos\theta_i \cos\theta_j}{\pi R^2} dA_i dA_j \tag{7}$$

The radiant heat-flux density ($\dot{q}_r$) among the heated surfaces and the other surfaces was calculated by means of Eq. 8 and then the radiative heat transfer coefficient was found through Eq. (9):

$$\dot{q}_{rad=} \sigma \sum_{j=1}^{n} F_{\varepsilon_{s-j}} \left(T_s^4 - T_j^4 \right) \tag{8}$$

$$h_r = \frac{q_r}{T_s - T_{AUST}} = \frac{\sigma \sum_{j=1}^{n} F_{\varepsilon_{s-j}} \left(T_s^4 - T_j^4\right)}{T_s - T_{AUST}} \quad (9)$$

Integral expression of the view factors in Eq. 6 was determined via a numerical approach using Matlab© code.

In the steps of calculation, the emissivity value of 0.8 has been employed for the ceiling surface. Besides, for the unheated surfaces the value of 0.9 has been input. It should be noted that these values were found by experimental methods, detailed in the previous section. The radiative heat transfer between entire surfaces was acquired by a 3D Matlab approach, in which the geometry along with surface temperatures were used. The total heat transfer coefficient (h_t) is acquired by the Eq. (10) as follows.

$$h_{tot} = \frac{\dot{q}_t}{T_{op} - T_s} \quad (10)$$

The convective heat transfer coefficient between the heated surfaces and room was determined by the equations below:

$$\dot{q}_c = \dot{q}_t - \dot{q}_r \quad (11)$$

$$h_c = \frac{\dot{q}_c}{T_s - T_a} \quad (12)$$

4. Computational Method

In order to solve the governing equations (continuity, momentum, and energy) the CFD software called FLUENT within the software ANSYS 14 is employed. It should be expressed that the summary of the program's solution way is established, in that, the control volume integral equations to be converted into algebraic equations. This process is conducted by realizing the integration of the related equations on the individual control volume and carrying out discretization of these equations [38].

From the options presented by the program, a turbulence model is chosen because all calculated Rayleigh number values are larger than 10^9. Also, to solve the equations more quickly, the first order upwind scheme was selected to discrete them. Generally, it is known that first order upwind scheme gives better convergence than the second one whereas it also gives less accuracy for tri/tet grids than hexagonal ones. In this study, all grids types are selected as hexagonal. The under relaxation elements pertaining to density, momentum, turbulence kinetic energy turbulence dissipation rate, turbulent viscosity and energy are selected as 1.0, 2.0, 0.8, 0.8, 1 and 0.9, correspondingly. The required duration for case studies to approximate to the solution has been found to be roughly 10 hours.

The residuals for momentum and continuity equations are selected to be 10^{-3}, whereas the value is 10^{-6} for energy equation. Also, properties of air in the room are calculated at the air temperature value in the middle of the enclosure in all cases, using the tables provided by Incropera and DeWitt [39].

One of two solvers provided by FLUENT, density based coupled solver is utilized. This solver concurrently solves relevant equations in vector form and additionally, pressure is drawn from the equation of state. Fig. 3 outlines the way followed in each iteration. Also, the Boussinesq methodology is chosen, since it greatly simplifies natural convection calculations that take place in governing equations. The k-ε RNG model is chosen, consistent with the recommendations made in a number of studies, such as the work of Seyam et al. [38].

The equation of continuity in Eq. (13), momentum in Eq. (14), and energy equation in Eq. (15) are given below for steady-state analyses:

$$\frac{\partial}{\partial x_i}\left(\rho u_i\right)=0 \tag{13}$$

$$\frac{\partial}{\partial x_i}\left(\rho u_i u_j\right)=-\frac{\partial p}{\partial x_i}+\frac{\partial}{\partial x_j}\left[\mu\left(\frac{\partial u_i}{\partial x_j}+\frac{\partial u_j}{\partial x_i}-\frac{2}{3}\delta_{ij}\frac{\partial u_l}{\partial x_l}\right)\right]+\frac{\partial}{\partial x_j}\left(-\rho\overline{u_i' u_j'}\right)+g_i\beta\left(T-T_0\right) \tag{14}$$

$$\frac{\partial}{\partial x_i}\left(\rho u_i h-\lambda\frac{\partial T}{\partial x_i}\right)=u_i\frac{\partial p}{\partial x_i}+\tau_{ij}\frac{\partial u_i}{\partial x_i} \tag{15}$$

where, S_{ij} and τ_{ij} are mean rate of strain tensor and viscous stress tensor, respectively as shown in Eqs. (16-17).

$$\tau_{ij}=2\mu S_{ij}-\frac{2}{3}\mu\frac{\partial u_l}{\partial x_l}\delta_{ij} \tag{16}$$

$$S_{ij}=\frac{1}{2}\left(\frac{\partial u_i}{\partial x_j}+\frac{\partial u_j}{\partial x_i}\right) \tag{17}$$

The RNG model has been derived via Re-Normalisation Group (RNG) techniques by Yakhot et al. [40] to renormalise the Navier-Stokes formulas, to take the influences of smaller scales of motion into account. The eddy viscosity is calculated through a single turbulence length scale in the standard k-epsilon model, for that reason the obtained turbulent diffusion is that which arises just at the certain scale, while all scales of motion will make contribution to the turbulent diffusion. The RNG method, a mathematical method, may be benefitted to develop a turbulence model similarly to the k-epsilon, outputs in a developed form of the

epsilon formula which efforts to consider the dissimilar scales of motion by means of alterations to the generation term.

There are numerous solutions to consider the transport formulas for k and ε, a basic interpretation where buoyancy is omitted is given below.

$$\frac{\partial}{\partial t}(\rho k)+\frac{\partial}{\partial x_i}(\rho k u_i)=\frac{\partial}{\partial x_j}\left[\left(\mu+\frac{\mu_t}{\sigma_k}\right)\frac{\partial k}{\partial x_j}\right]+P_k-\rho\varepsilon \tag{18}$$

$$\frac{\partial}{\partial t}(\rho\varepsilon)+\frac{\partial}{\partial x_i}(\rho\varepsilon u_i)=\frac{\partial}{\partial x_j}\left[\left(\mu+\frac{\mu_t}{\sigma_\varepsilon}\right)\frac{\partial \varepsilon}{\partial x_j}\right]+C_{1\varepsilon}\frac{\varepsilon}{k}P_k-C_{2\varepsilon}^{*}\rho\frac{\varepsilon^2}{k} \tag{19}$$

where,

$$C_{2\varepsilon}^{*}=C_{2\varepsilon}+\frac{C_\mu\eta^3(1-\eta/\eta_0)}{1+\beta\eta^3} \tag{20}$$

$$S=(2S_{ij}S_{ij})^{1/2} \tag{21}$$

$$\eta=Sk/\varepsilon \tag{22}$$

$$S=(2S_{ij}S_{ij})^{1/2} \tag{23}$$

$$\beta=0.012 \tag{24}$$

With the turbulent viscosity being predicted similarly with the standard k-epsilon model. The RNG k-ε model, used in this analyses, is proposed for indoor air simulations.

4.1 Grid generation

Gaining valid outcomes of a natural convection problem through a CFD program firstly depends on appropriately meshing of the examined body. To succeed in this goal, the program named Design Modeler within ANSYS 14, is chosen. As pointed out by the program producer, in basic geometries such as the system in this work, the quad/hex meshes bring about more reliable results than those of obtained by a tri/tet option. For this reason, quad/hex meshing is selected. Because of fast temperature variations at air layers next to walls, meshing frequency has been chosen to be dense near surfaces, yet less dense as getting far from walls, as shown in Fig. 4. This situation has also arisen from the fact that no temperature difference is seen between outside thermal boundary layer and center of the room.

4.2 Thermal boundary conditions

Journal Pre-proofs

To investigate the effect of temperature difference between the radiant surface and air on convection and heat flux rates, computational case works have been performed at reasonable surface temperatures (T_s= 30-50^{o}C, T_w= 15-24^{o}C, T_f= 15-24^{o}C), at constant room dimensions same with that of experimental chamber detailed in Section 2 (LxHxW= 4x3x4 m). It should be noted that in the CFD model thermal boundary conditions of room surfaces have been chosen as inputs (in particular, ceiling surface temperature varying between 30^{o}C and 50^{o}C with 5^{o}C intervals), while emissivity of walls and floor selected as 0.9 and ceiling varying between 0.8 and 0.9. Similar to real hydronic radiant heating and cooling applications, in the simulations, a constant surface temperature preference is applied for radiant room surfaces. The gravitational force is input to the software as -9.81 m/s^2 in the y direction in Fig. 4.

4.3 Independency of outputs from grids

A point of utmost significance in employing a CFD program and thus acquiring outcomes in this way, is to diminish the effect of meshing structure on the results obtained. To be sure on if the effect of meshing structure is adequately reduced, the Nusselt numbers are drawn by the software's area weighted average specialty. It should be seen that the Nusselt number over the heated surface indicates to total convective heat transfer through the surface and is evaluated as a benchmark in this regard, as well. Varying interval numbers at x, y and z axes make up different total cell numbers in the room and can be seen in Table 3. It is evident that valid for the identical thermal boundary conditions, if the total cell number rises from 50625 to 90750, the Nusselt number varies less than 1%. In addition, because the outcomes pertaining to the presented meshing numbers are so close, the meshing combination next to the last one, corresponding to 50625 cells is found to be the appropriate option, and hence it is concluded that the influence of cell counts on the outcomes have been eliminated. From this perspective, the numerical cases have been conducted with chosen mesh numbers.

5. ANN Method

Artificial neural networks are preferable prediction approaches among a lot of other applications. Selected physical problems/cases can be analyzed easily by means of using artificial neural networks precisely. ANN approaches have the ability of solving the time consuming problems more quickly than the other estimation methods. Due to the high adaptive capacity of ANNs, insufficient data may be predicted in a reliable way. As a study conducted by Olofsson and Anderson [28], via artificial neural networks they predicted long term energy demand with considering short term demand. Besides, a well-constructed ANN structure can enhance the reliability of radiant system's performance assessments. From this perspective, an ANN approach, which has been explained in this section, is applied to the current radiant heated ceiling system. Different neural network structures were employed and the most successful networks were selected in this study. Two different neural networks were generated for heat fluxes and heat transfer coefficients. Inputs

for the both neural networks were T_s, T_s-T_a and AUST while the outputs were q_r and q_t and, h_r, h_c and h_t for heat flux and heat transfer coefficient networks respectively. All inputs and outputs were normalized in network processes. Different number of hidden layer neurons was applied for all network structures to observe the prediction performance and to obtain the best network. Different set of transfer function pairs were also employed for all tested neural networks. These transfer functions were tansig, logsig and purelin and it should also be noted that the purelin transfer function was used on output layer only. Nguyen-Widrow procedure was employed to weights and biases in order to obtain fast convergence. Levenberg-Marquardt training function was employed to all tested networks since it demonstrated its capability in numerous prediction problems in heat transfer area.

Overfitting may occur in neural networks and reduce overall generalization ability. Therefore, convergence criteria was limited to prevent the network from overfitting the outputs and performance of the networks were monitored during training and validation phase. Performance evaluation of the neural networks was conducted with mean square error (MSE), and coefficient of determination (R^2) is given as follows:

$$\mathrm{MSE} = \frac{1}{\mathrm{n}} \sum_{\mathrm{i}=1} \left(\mathrm{f_i} - \mathrm{y_i} \right)^2 \tag{25}$$

$$R^2 = 1 - \frac{SS_{res}}{SS_{tot}} \tag{26}$$

$$\mathrm{SS}_{res} = \sum_{\mathrm{i}=1} \left(\mathrm{y_i} - \mathrm{f_i} \right)^2 \tag{27}$$

$$\mathrm{SS}_{tot} = \sum_{\mathrm{i}=1} \left(\mathrm{y_i} - \overline{y} \right)^2 \tag{28}$$

f_i, y_i, n and $\overline{y}$ were defined as predicted value, experimental value, pattern number and the average value of experimental values correspondingly.

6. Results and Discussion

The current study presents the heat flux and heat transfer coefficient data of a heating by ceiling application within a room, collected by means of measurements in an experimental chamber and a CFD study of which calculation steps were elaborated in Sections 2 – 4. Using the program's area weighted average selection, the convective heat transfer coefficients, and Nusselt numbers are obtained. It should be noted that as well as 28 experimental tests, 46 CFD case studies were conducted to seize a sufficient number of data set for an ANN application, which is a similar amount to authors' publication [29]. The thermal boundary conditions

applied in the case studies have been chosen as reasonable surface temperatures that can be met in a radiant ceiling heating preference. Additionally, as well as the measurements from the experimental chamber, detailed heat flux and heat transfer coefficient data acquired from experimental and CFD work were given in Tables 4 and 5, respectively.

The reason of coming up with an ANN application by having an adequate number of data number is to explore and suggest a new path to predict heat fluxes and heat transfer coefficients arising over these kind of systems. To this end, 150 different neural network structures were tested in total and the best outcomes for heat flux and heat transfer coefficient networks were presented in Table 6. All subsequent calculations in the study were made with these two neural networks. Weights and biases of the neural network were illustrated in Table 7 and 8 for heat flux and heat transfer coefficient respectively. IW, LW and B represent input weight, layer weight and bias respectively. Neural network results can be represented with matrices as follows:

$$Y = tansig\left(B_2 + LW.tansig\left(B_1 + IW.X\right)\right) \tag{29}$$

In Eq. 17, Y and X represent output and input matrix respectively. It should also be noted that the current neural networks use inputs and outputs normalized between -1 and 1. Inputs should be sorted as T_s, T_s-T_a and T_s-AUST in order to acquire correct results. Output sequences are q_r, $q_{t,}$ and h_r, h_c, h_t for heat flux and heat transfer coefficient respectively.

Furthermore, to demonstrate the success of the newly developed ANN approach, contrasting the results of it with experimentally obtained outcomes, is a necessity. To achieve this, in Fig. 5a and 5b, the radiative and total heat flux outcomes of the ANN application are compared with those calculated from experimental measurements. It is noticeable from these figures that for both radiative and total heat flux ANN results, they stay in a very tolerable range of 15% and thus it is evident that the novel approach progressed in the present paper has accomplished the goal of accurately providing the heat flux values of radiant ceiling heating.

In order to validate the CFD analyses by experimental data have been selected randomly among 28 experimental data points. Then, ANSYS Fluent software has been run with Boussinesq and k-ε RNG models and Figs. 6 a-b have been obtained as a result. The deviation bands became ±10% for q_r and ±5% for q_t in these figures. It should be noted that detailed analyses on the derivation of total heat transfer coefficient using these experimental data were given in authors' previous publication [36].

In Fig. 7a, radiative heat transfer coefficient values are compared with ones found by means of ANN approach. Just as in Fig. 5a pertaining to radiative heat flux data, in Fig. 7a the radiative heat transfer

coefficient results are estimated in a 15% deviation range, by the ANN. It should be seen that while calculating the radiative heat transfer coefficients from experimental data, a theoretical method, called net-radiosity method is employed and hence unlike convective results no reason exists to cause ANN method's outputs to deviate more.

Fig. 7b illustrates the comparison of the results of ANN method with experimentally obtained results. While a significant part of the points in the figure remain within a 15% interval, which is a very credible deviation value, there are also data points lying out of this range by 30%. As mentioned in the interpretation of Fig. 7a, this higher proportion of deviation range may be accounted for the fact that possibly and unavoidable measurement errors met in the experimental measurements are only assigned to convective heat transfer calculations. Therefore, this may lead predictions of ANN method to deviate and some of the estimations of ANN approach to be between the deviation range of 15% and 30%, as well.

Fig. 7c reveals the comparison of total heat transfer coefficients acquired by ANN method with ones determined through experimental setup and measurements. It is clear that an overwhelming portion of points lies within a very credible 15% deviation range and this proves the success of the progressed ANN approach regarding with determination of total heat transfer coefficients occurring over a heated ceiling. Few points on this figure remain out of this successful deviation range by the 30% deviation ratio. This may be attributed to presumable unavoidable experimental measurement errors influencing convective calculations which are also encompassed by total heat transfer coefficient, and also their slight effect on ANN calculation process.

From Figs. 7a and 7b, it can be understood that the radiative and convective heat transfer coefficients mean values are 5.3 W/m^2K and 0.9 W/m^2K, respectively. Awbi and Hatton [4] and Causone et al. [17] have calculated the convective heat transfer coefficient as 0.5 W/m^2K and 0.3 W/m^2K, respectively. In a heated radiant ceiling applications, warmer air over the heated surface confronts with the cool room air, nevertheless, rising nature of the warmer air than that of the cool room air is thwarted by the ceiling. Thus, less air movements are generated in comparison to a radiant heated wall or a floor and hence lower values of convective heat flux are found. The values obtained by these researches show very close values to each other. According to EN 1264-5 [31], the total heat transfer coefficients of heated radiant ceiling are obtained to be 6.5 W/m^2K. In the current work, total heat transfer coefficient is found as 7.0 W/m^2K meanly using dissimilar 74 ANN investigations as illustrated in Fig. 7c. This value is not a far one from the proposal of EN 1264-5 [31]. It should be noted that Causone et al. [17] have found it as 5.8 W/m^2K for the similar operating conditions. Hence, these minor deviations may be considered as a comparison for the validity of the present work.

Figs. 8 (a-d) provide a number of contours and vectors, when the thermal boundary conditions of (T_s= 50^{o}C, T_w= 24^{o}C, and T_f= 18^{o}C) are applied to the numerically modeled office, of which room dimensions are

indicated in previous sections. These figures not only give the physical mechanism of the investigated subject, but also they show the CFD analyses accuracy since they have been obtained expectedly from CFD. It is clear from Fig. 8a that HRC results in an equal thermal stratification beside the ceiling region, and by the region next to the floor surface temperature contour remains constant, while air having lowest temperature remains on the floor. Fig. 8b illustrates velocity vectors within the examined chamber, and it is obvious that over walls highest velocity magnitudes have happened. Fig. 8c demonstrates radiant heat flux vectors in the chamber. It is understandable that radiant heat flux vectors over the ceiling are of the highest values, as flux vectors in the midst of ceiling are less strong. It can also be noticed that walls and floor have negative flux values different than those of the ceiling. Additionally, Fig 8d presents surface heat transfer coefficients as vectors on surfaces. It can be deduced that through the figure that is in compliance with the outcomes presented by figures and tables, the greatest heat transfer coefficients are acquired over the ceiling, and it ought to be added that the coefficient values encompass both convective and radiative heat transfer from the ceiling.

7. Conclusion

The present work aims to present a comprehensive analyzing method to eliminate the discrepancies between proposed and actual values of heat fluxes and heat transfer coefficients happening in radiant systems. The paper shows comparison between experimental data obtained with those of the artificial neural network approach progressed by benefitting from experimental and numerical inputs and outputs. It should be specified that experiments were carried out within a room heated from its ceiling at various supply water temperatures and thus ceiling temperatures. After obtaining experimental data, at reasonable surface boundary conditions a computational study was conducted to increase the number of data to make it sufficient for an artificial neural network application and also to validate the experimental results. Moreover, artificial neural network investigations were implemented by choosing surfaces temperatures and corresponding temperature difference reference values determined in the relevant literature as inputs, and radiative and total heat fluxes and heat transfer coefficients as outputs. This technique on the increase of insufficient test data number by means of a commercial software should be used by others in the literature. The used artificial neural network method in the present work is supposed to be common one in the near future. Concise conclusions deduced through the study can be summarized as follows:

a. For a radiant ceiling heating application's heat flux values and heat transfer coefficients, 22 neurons and 7 neurons network structures have given the most successful results with tansig transfer functions, of which correlations constants are presented in detail.

b. Similar to various heat transfer applications in the relevant literature, Levenberg-Marquardt function has provided the best results.

c. From the experimental database belonging to a radiant ceiling heating application, mean heat transfer coefficient results of 0.9 W/m^{2}K, 5.3 W/m^{2}K, and 7.0 W/m^{2}K are found for convective, radiative, and total heat transfer coefficients, correspondingly.

d. The developed and elaborated artificial neural network approach is capable of estimating an overwhelming part of heat flux and heat transfer characteristics of a ceiling heating system, within a deviation range of 15%.

e. A significant amount of experimental and computational data sets have been acquired for the relevant literature and validation purposes of other researchers.

f. A novel approach in order to study the heat transfer characteristics of radiant heated ceiling system has been proposed by means of the analyses of computational fluid dynamics and artificial neural networks for the sake of other researchers who can also adapt this idea to various research subjects.

Nomenclature

A : surface area of the panel (m^2)

B : bias

ANN : artificial neural network

AUST : average unheated surface temperature (^{o}C)

CFD : computational fluid dynamics

c_p : specific heat (J/kgK)

ε : surface emissivity

F_{s-j} : view factor between the radiant surface and j surfaces

f_i : predicted value

HRC : heated radiant ceiling

HTCs : heat transfer coefficients

IW : input weight

h_c : convective heat transfer coefficient (W/m^{2}K)

h_r : radiative heat transfer coefficient (W/m^{2}K)

h_t : overall heat transfer coefficient (W/m^{2}K)

LW : layer weight

Journal Pre-proofs

m_w : mass flow rate (kg/s)

MSE : mean square error

n : pattern number

Q_c : convective heat transfer (W)

Q_{loss} : conduction heat loss (W)

Q_t : total heat transfer from panels (W)

Q_r : radiative heat transfer (W)

q_c : convective heat flux (W/m^2)

q_r : radiative heat flux (W/m^2)

q_t : total heat flux (W/m^2)

R : correlation coefficient

T_a, T_{op}, T_s, T_w, T_f, $T_{w,1}$, $T_{w,2}$: air temperature, operative temperature, heated surface temperature, wall temperature, floor temperature, water inlet temperature, water outlet temperature (^oC)

U : thermal transmittance coefficient of surfaces (W/m^2K)

X : input matrix

Y : output matrix

y_i : experimental value

$\bar{y}$: mean value of experimental values

ΔT : temperature difference between radiant heated wall and reference temperature at corresponding heat transfer coefficients (^oC)

Acknowledgement

The current work has been economically sustained by Yildiz Technical University Scientific Research Projects Coordination Department, Project Number: FBA-2019-3743. The seventh author acknowledges the financial support provided by the "Research Chair Grant" National Science and Technology Development Agency (NSTDA) and King Mongkut's University of Technology Thonburi through the "KMUTT 55th Anniversary Commemorative Fund".

Journal Pre-proofs

References

[1] F. Mancini, G. Lo Basso, De Santoli, L. Energy use in residential buildings: Impact of building automation control systems on energy performance and flexibility. Energies, 12-15 (2019) 2896.

[2] ASHRAE HVAC Systems and Equipment Handbook, Chapter 6: Panel Heating and Cooling, American Society of Heating Refrigeration and Air-conditioning Engineers, USA, (2000).

[3] G. N. Walton, A new algorithm for radiant interchange in room loads calculations, ASHRAE Tran. 86 (2) (1980) 190-208.

[4] H.B. Awbi, A. Hatton, "Natural convection from heated room surfaces," Energy Build. 30, vol. 7788, no. August, pp. 233–244, 1999.

[5] O. Acikgoz, Y. Karakoyun, Z. Yumurtacı, N. Dukhan, A. S. Dalkılıç, Realistic experimental heat transfer characteristics of radiant floor heating using sidewalls as heat sinks, Energy and Buildings. 183 (2019) 515-526.

[6] O. Acikgoz, Y. Karakoyun, Z. Yumurtacı, A. S. Dalkılıç, An experimental investigation on heat transfer characteristics arising over an underfloor cooling system exposed to different radiant heating loads through walls. Applied Thermal Engineering 164 (2020) 114517.

[7] Liu, J., & Lin, Z. (2020). Energy and Exergy Performances of Floor, Ceiling, Wall Radiator and Stratum Ventilation Heating Systems for Residential Buildings. Energy and Buildings, 110046.

[8] Lateb, M., & Fellouah, H. (2019). Duty Cycle of a Radiant Ceiling Heating System under Extremely Cold-Temperature Conditions: A Theoretical Assessment. Journal of Energy and Power Engineering, 13, 359-368.

[9] M. Bojić, D. Cvetković, V. Marjanović, M. Blagojević, and Z. Djordjević, "Performances of low temperature radiant heating systems," Energy Build., vol. 61, pp. 233–238, 2013.

[10] K. Zhao, X. H. Liu, Y. Jiang, On-site measured performance of a radiant floor cooling/heating system in Xi'an Xianyang International Airport, Solar Energy. 108 (2014) 274-286.

[11] Safizadeh, M. R., Watly, L., & Wagner, A. (2019). Evaluation of Radiant Heating Ceiling Based on Energy and Thermal Comfort Criteria, Part II: A Numerical Study. Energies, 12(18), 3437.

[12] Fanger, P.O., Banhidi, L., Olesen, B.W., Langkilde, G. Comfort limits for heated ceilings. ASHRAE Trans. 1980, 86, 141–156.

[13] Safizadeh, M. R., Schweiker, M., & Wagner, A. (2018). Experimental evaluation of radiant heating ceiling systems based on thermal comfort criteria. Energies, 11(11), 2932.

[14] Yuan, Y., Zhou, X., & Zhang, X. (2019). Numerical and experimental study on the characteristics of radiant ceiling systems. Building Research & Information, 47(8), 912-927.

[15] Miriel, J., Serres, L., & Trombe, A. (2002). Radiant ceiling panel heating–cooling systems: experimental and simulated study of the performances, thermal comfort and energy consumptions. Applied Thermal Engineering, 22(16), 1861-1873.

[16] Koca, A., & Çetin, G. (2017). Experimental investigation on the heat transfer coefficients of radiant heating systems: Wall, ceiling and wall-ceiling integration. Energy and Buildings, 148, 311-326.

[17] Causone, F., Corgnati, S. P., Filippi, M., & Olesen, B. W. (2009). Experimental evaluation of heat transfer coefficients between radiant ceiling and room. Energy and buildings, 41(6), 622-628.

[18] Yuan, Y., Zhang, X., & Zhou, X. (2017). Simplified correlations for heat transfer coefficient and heat flux density of radiant ceiling panels. Science and Technology for the Built Environment, 23(2), 251-263.

[19] Cholewa, T., Anasiewicz, R., Siuta-Olcha, A., & Skwarczynski, M. A. (2017). On the heat transfer coefficients between heated/cooled radiant ceiling and room. Applied Thermal Engineering, 117, 76-84.

[20] R. Li, T. Yoshidomi, R. Ooka, B. W. Olesen, Field evaluation of performance of radiant heating/cooling ceiling panel system, Energy and Buildings. 86 (2015) 58-68.

[21] R. Hu, and J. L. Niu, A review of the application of radiant cooling & heating systems in Mainland China, Energy and Buildings. 52 (2012) 11-19.

[22] J. Shinoda, O. B. Kazanci, S. I. Tanabe, B. W. Olesen, A review of the surface heat transfer coefficients of radiant heating and cooling systems. Building and Environment, 159 (2019) 106156.

[23] Zhang, T., Liu, Y., Rao, Y., Li, X., & Zhao, Q. (2020). Optimal design of building environment with hybrid genetic algorithm, artificial neural network, multivariate regression analysis and fuzzy logic controller. Building and Environment, 106810.

[24] Jihad, A. S., & Tahiri, M. (2018). Forecasting the heating and cooling load of residential buildings by using a learning algorithm "gradient descent", Morocco. Case studies in thermal engineering, 12, 85-93.

[25] Yokoyama, R., Wakui, T., & Satake, R. (2009). Prediction of energy demands using neural network with model identification by global optimization. Energy Conversion and Management, 50(2), 319-327.

[26] Benedetti, M., Cesarotti, V., Introna, V., & Serranti, J. (2016). Energy consumption control automation using Artificial Neural Networks and adaptive algorithms: Proposal of a new methodology and case study. Applied Energy, 165, 60-71.

[27] Pino-Mejías, R., Pérez-Fargallo, A., Rubio-Bellido, C., & Pulido-Arcas, J. A. (2017). Comparison of linear regression and artificial neural networks models to predict heating and cooling energy demand, energy consumption and CO2 emissions. Energy, 118, 24-36.

[28] Olofsson, T., & Andersson, S. (2001). Long-term energy demand predictions based on short-term measured data. Energy and Buildings, 33(2), 85-91.

[29] Acikgoz, O., Çebi, A., Dalkilic, A. S., Koca, A., Çetin, G., Gemici, Z., & Wongwises, S. (2017). A novel ANN-based approach to estimate heat transfer coefficients in radiant wall heating systems. Energy and Buildings, 144, 401-415.

[30] Karadağ, R., & Akgöbek, Ö. (2008). The prediction of convective heat transfer in floor-heating systems by artificial neural networks. International Communications in Heat and Mass Transfer, 35(3), 312-325.

[31] EN 1264-5, Water Based Surface Embedded Heating and Cooling Systems – Part 5: Heating and Cooling Surfaces Embedded in Floors, Ceilings and Walls, 2008.

[32] BS EN 14037-1, Free hanging heating and cooling surfaces for water with a temperature below 120°C. Pre-fabricated ceiling mounted radiant panels for space heating. Technical specifications and requirements, 2016.

[33] A. Koca, Z. Gemici, Y. Topacoglu, G. Cetin, R.C. Acet, B.B. Kanbur, Experimental investigation of heat transfer coefficients between hydronic radiant heated wall and room, Energy and Buildings 82 (2014) 211-221.

[34] Standard 138-2013, Method of Testing for Rating Ceiling Panels for Sensible Heating and Cooling (ANSI Approved), 2016.

[35] ANSI/ASHRAE Standard 55, Thermal Environmental Conditions for Human Occupancy, 2016.

[36] Koca, A., Acikgoz, O., Çebi, A., Çetin, G., Dalkilic, A. S., & Wongwises, S. (2018). An experimental investigation devoted to determine heat transfer characteristics in a radiant ceiling heating system. Heat and Mass Transfer, 54(2), 363-375.

[37] BS EN 14240, Ventilation for buildings. Chilled ceilings. Testing and rating, 2004.

[38] S. Seyam, A. Huzayyin, H. El-Batsh, S. Nada, Experimental and numerical investigation of the radiant panel heating system using scale room model, Energy and Buildings. 82 (2014) 130-141.

[39] F.P. Incropera, D.P. DeWitt, Fundamentals of heat and mass transfer. 4th ed. New York: Wiley & Sons; 1996.

[40] Yakhot, V. S. A. S. T. B. C. G., Orszag, S. A., Thangam, S., Gatski, T. B., & Speziale, C. G. (1992). Development of turbulence models for shear flows by a double expansion technique. Physics of Fluids A: Fluid Dynamics, 4(7), 1510-1520.

Journal Pre-proofs

Table 1: Controlled factors in the conditioned rooms

	Ceiling	Floor	Facade Room	Interior Room
Temperature Range	-10˚C / +40˚C	+0˚C / +30˚C	-10˚C / +40˚C	+0˚C / +30˚C
Temperature Tolerance	± 0.5 ˚C	± 0.5 ˚C	± 0.5 ˚C	± 0.5 ˚C
Humidity Range	n/a	n/a	%35 / %85 RH	n/a
Humidity Control Steps	n/a	n/a	%1	n/a
Humidity Tolerance	n/a	n/a	± % 0.5 RH	n/a
Air Velocity	n/a	n/a	0.5 – 5 m/s	n/a

Journal Pre-proofs

Table 2 Coefficient of thermal transmittance of surfaces

Surfaces	**U (W/m²K)**
Ceiling	0.3
Floor	0.4
North Wall	0.4
West Wall	0.4
East Wall	0.8
South Wall	0.8

Journal Pre-proofs

Table 3 The alteration of Nusselt number as the number of cells within the cavity change

Combinations of interval counts in x-y-and z axes	**Number of cells**	**Nusselt number**
20x20x20	8000	140.01
35x20x35	24500	141.87
45x25x45	50625	142.56
55x30x55	90750	142.94

Journal Pre-proofs

Table 4 Results obtained from CFD work

Case study no	q_t	q_r	q_c	T_s	T_a	T_s-T_a	T_w	T_f	AUST	T_s-AUST	h_c	h_t	h_r
1	95,85	80,81	15,04	35	22,3	12,7	20	20	20	15	1,18	7,55	5,39
2	111,87	94,68	17,19	35	20,08	14,92	18	15	17,23	17,77	1,15	7,50	5,33
3	107,5	90,69	16,81	35	20,54	14,46	18	18	18	17	1,16	7,43	5,33
4	102,92	86,57	16,35	35	21,06	13,94	18	21	18,79	16,21	1,17	7,38	5,34
5	89,9	75,79	14,11	35	23,19	11,81	21	21	21	14	1,19	7,61	5,41
6	76,44	64,68	11,76	35	25,27	9,73	24	21	23,23	11,77	1,21	7,86	5,50
7	124,32	105,13	19,19	35	17,86	17,14	15	15	15	20	1,12	7,25	5,26
8	90,8	76,84	13,96	30	17,11	12,89	15	15	15	15	1,08	7,04	5,12
9	78,38	66,39	11,99	30	19,34	10,66	18	15	17,23	12,77	1,12	7,35	5,20
10	74,02	62,4	11,62	30	19,79	10,21	18	18	18	12	1,14	7,25	5,20
11	69,41	58,29	11,12	30	20,33	9,67	18	21	18,79	11,21	1,15	7,18	5,20
12	56,41	47,51	8,9	30	22,43	7,57	21	21	21	9	1,18	7,45	5,28
13	42,95	36,39	6,56	30	24,48	5,52	24	21	23,23	6,77	1,19	7,78	5,38
14	38,15	32,15	6	30	25,02	4,98	24	24	24	6	1,20	7,66	5,36
15	86,49	72,85	13,64	30	17,56	12,44	15	18	15,79	14,21	1,10	6,95	5,13
16	64,61	54,04	10,57	30	21,11	8,89	18	24	19,6	10,4	1,19	7,27	5,20
17	51,6	43,26	8,34	30	23,03	6,97	21	24	21,79	8,21	1,20	7,40	5,27
18	106,67	90,13	16,54	40	26,56	13,44	24	24	24	16	1,23	7,94	5,63
19	111,45	94,38	17,07	40	26,04	13,96	24	21	23,23	16,77	1,22	7,98	5,63
20	124,91	105,49	19,42	40	23,94	16,06	21	21	21	19	1,21	7,78	5,55
21	120,14	101,25	18,89	40	24,47	15,53	21	24	21,79	18,21	1,22	7,74	5,56
22	137,93	116,27	21,66	40	21,81	18,19	18	21	18,79	21,21	1,19	7,58	5,48
23	133,16	112,03	21,13	40	22,36	17,64	18	24	19,6	20,4	1,20	7,55	5,49
24	146,88	124,38	22,5	40	20,83	19,17	18	15	17,23	22,77	1,17	7,66	5,46
25	142,5	120,39	22,11	40	21,3	18,7	18	18	18	22	1,18	7,62	5,47
26	133,9	113,6	20,3	40	22,99	17,01	21	15	19,48	20,52	1,19	7,87	5,54
27	120,48	102,48	18	40	25,1	14,9	24	15	21,74	18,26	1,21	8,09	5,61
28	143,22	121,29	21,93	45	27,33	17,67	24	24	24	21	1,24	8,11	5,78

Journal Proofs

Table 4 Results obtained from CFD work (cont.)

Case study no	q_t	q_r	q_c	T_s	T_a	T_s-T_a	T_w	T_f	AUST	T_s-AUST	h_c	h_t	h_r
29	147,99	125,54	22,45	45	26,81	18,19	24	15	21,74	23,26	1,23	8,14	5,40
30	156,68	132,41	24,27	45	25,23	19,77	21	24	21,79	23,21	1,23	7,93	5,70
31	174,47	147,43	27,04	45	22,57	22,43	18	21	18,79	26,21	1,21	7,78	5,62
32	161,44	136,65	24,79	45	24,71	20,29	21	21	21	24	1,22	7,96	5,69
33	169,73	143,19	26,54	45	23,07	21,93	18	24	19,6	25,4	1,21	7,74	5,64
34	166,03	140,77	25,26	45	24,21	20,79	21	18	20,23	24,77	1,22	7,99	5,68
35	152,59	129,65	22,94	45	26,33	18,67	24	18	22,48	22,52	1,23	8,17	5,76
36	181,32	153,95	27,37	50	27,1	22,9	24	24	24	26	1,20	7,92	5,92
37	147,99	125,54	22,45	50	26,81	23,19	24	21	23,23	26,77	0,97	6,38	4,69
38	190,69	162,31	28,38	50	27,1	22,9	24	18	22,48	27,52	1,24	8,33	5,90
39	166,03	140,77	25,26	50	24,21	25,79	21	18	20,23	29,77	0,98	6,44	4,73
40	71,66	60,43	11,23	35	25,79	9,21	24	24	24	11	1,22	7,78	5,49
41	85,12	71,55	13,57	35	23,73	11,27	21	24	21,79	13,21	1,20	7,55	5,42
42	98,13	82,33	15,8	35	21,7	13,3	18	24	19,6	15,4	1,19	7,38	5,35
43	94,49	79,91	14,58	35	22,68	12,32	21	18	20,23	14,77	1,18	7,67	5,41
44	81,04	68,79	12,25	35	24,78	10,22	24	18	22,48	12,52	1,20	7,93	5,49
45	98,89	83,9	14,99	35	22,23	12,77	21	15	19,48	15,52	1,17	7,74	5,41
46	85,46	72,79	12,67	35	24,33	10,67	24	15	21,74	13,26	1,19	8,01	5,49

Journal Pre-proofs

Table 5 Experimental results obtained from measurements in experimental setup

Case study no	q_t	q_r	q_c	T_s	T_a	T_s-T_a	T_w	T_f	T_{AUST}	T_s-T_{AUST}	h_c	h_t	h_r
1	35,2	30,6	4,6	25,8	20	5,8	19,54	18,43	19,2	6,6	0,8	6,5	4,6
2	35,2	30,5	4,8	25,7	19,3	6,4	19,89	18,54	19,4	6,3	0,8	6,1	4,8
3	37,4	32,8	4,6	25,8	19,6	6,2	20,22	18,66	19,6	6,2	0,7	6,6	5,2
4	34,6	30	4,6	25,8	19,8	6	20,53	18,78	19,8	6	1	6,8	5,1
5	35,4	30,8	4,6	25,8	20	5,8	20,80	18,91	20	5,8	0,9	6,9	5,2
6	35,9	31,3	4,7	25,8	20	5,8	20,67	18,78	19,9	5,9	0,9	6,7	5,3
7	35,8	31,3	4,5	25,8	20	5,8	20,16	18,81	19,6	6,2	0,8	6,7	5,1
8	46,4	40,6	5,8	30,9	23,1	7,8	23,43	21,87	23	7,9	0,9	6,8	5,1
9	45,1	39	6,1	30,8	22,8	8	23,27	21,57	22,7	8,1	0,8	6,4	4,8
10	46,8	41	5,8	31,1	23,1	8	23,74	21,96	23,1	8	0,8	6,9	5,4
11	45,3	39,4	5,8	31	23,1	7,9	23,97	22,11	23,3	7,7	0,8	6,7	5,3
12	45,9	40,3	5,7	31,1	23,4	7,7	23,90	21,94	23,2	7,9	0,8	6,7	5,2
13	46	40,1	5,9	30,9	23,3	7,6	23,83	21,87	23,1	7,8	0,9	6,7	5,2
14	47,1	41	6	30,9	23,2	7,7	23,48	21,78	22,9	8	0,8	6,8	5,2
15	55,7	48,9	6,9	36	26,9	9,1	24,40	22,34	26,8	9,2	0,7	6,7	5,3
16	56	49,1	6,9	35,9	26,7	9,2	27,19	25,16	26,6	9,3	0,8	6,7	5,3
17	56,4	49,8	6,6	35,9	26,5	9,4	27,01	24,97	26,4	9,5	0,7	6,5	5,3
18	57,2	50,4	6,7	36	26,3	9,7	26,82	24,83	26,3	9,7	0,6	6,8	5,2
19	57	50	7	35,9	26,4	9,5	26,66	24,66	26,1	9,8	0,8	6,6	4,9
20	55,5	48,9	6,6	36	26,5	9,5	26,95	24,91	26,4	9,6	0,7	6,6	5,1
21	56,2	49,5	6,7	36,2	26,6	9,6	27,31	25,32	26,4	9,8	0,7	6,7	5,4
22	67,7	60,3	7,4	43	32,5	10,5	31,73	28,37	31	12	0,5	6,4	4,9
23	69,5	62	7,5	43,1	32,3	10,8	31,58	28,20	31,9	11,2	0,6	6,6	5,5
24	70	62,3	7,7	43	32,2	10,8	32,45	29,04	31,3	11,7	0,7	6,6	5,3
25	68,2	60,5	7,7	42,9	32,1	10,8	32,32	28,87	31,6	11,3	0,5	6,6	5,4
26	68,6	61,1	7,5	43	32	11	32,23	28,76	31,4	11,6	0,6	6,1	5,1
27	67,8	60,1	7,8	43,1	31,8	11,3	31,95	28,54	31,2	11,9	0,5	6,2	5,1
28	70,3	62,6	7,7	43,2	32,3	10,9	32,13	28,77	31,4	11,8	0,6	6,6	5,2

Journal Proofs

Table 6 Performance of best neural networks for heat flux and heat transfer coefficient

	Network Structure	Transfer Functions	R^2		
			q_r	q_t	
Heat flux	22 neurons	Tansig-Tansig	0.9991	0.9992	
			h_r	h_c	h_t
Heat transfer coefficient	7 neurons	Tansig-Tansig	0.8435	0.9666	0.9680

Journal Pre-proofs

Table 7 Weight and bias matrix for heat flux outputs

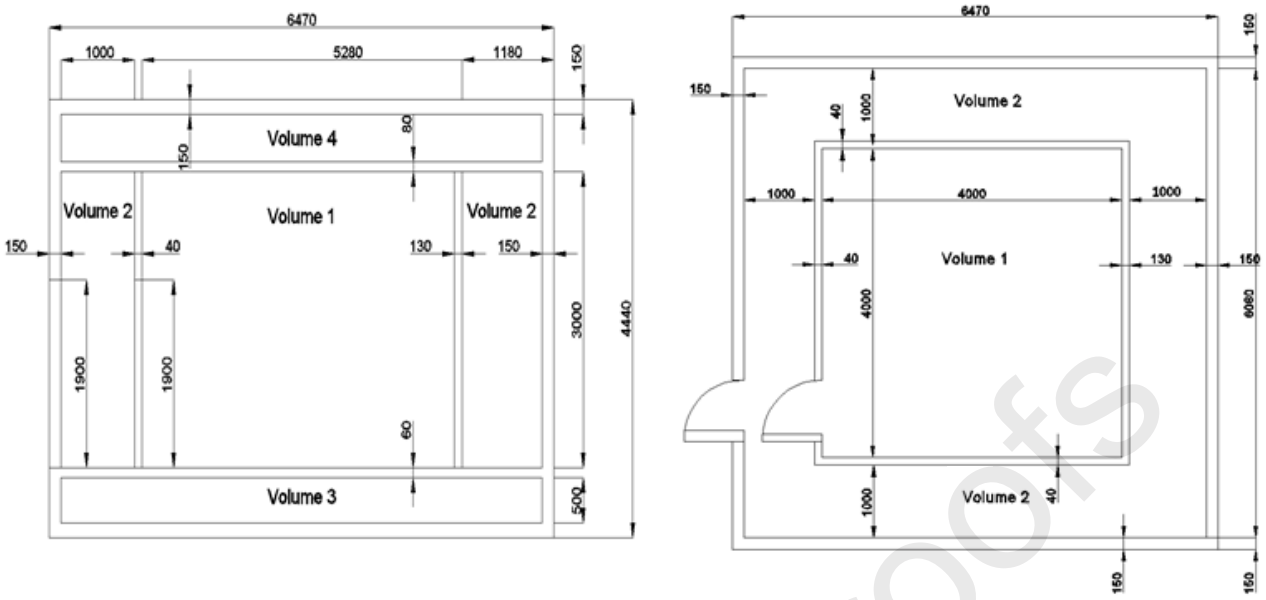
$$IW = \begin{bmatrix} 0.13672 & -7.97157 & -0.43363 \\ -1.09273 & -3.11634 & -2.45101 \\ -2.23832 & -3.11373 & -0.81851 \\ 0.83192 & -3.07045 & 2.24145 \\ -1.12584 & -1.08347 & 2.97945 \\ -1.49708 & -3.72575 & 0.38873 \\ 0.04481 & 2.15130 & 3.17984 \\ -1.08175 & -3.33942 & -1.05710 \\ 4.34110 & 0.17126 & -1.66498 \\ 3.60314 & -2.14209 & 2.04335 \\ 3.14277 & 0.81689 & -0.75864 \\ -1.63486 & 0.64835 & 4.34431 \\ 1.72990 & 0.64912 & -3.66127 \\ 3.37006 & 0.67383 & 1.73690 \\ 0.78141 & -1.22578 & -3.67070 \\ -2.79794 & 2.00057 & 1.23647 \\ 2.73591 & 2.71011 & 2.78669 \\ 2.46584 & -1.39253 & 2.33510 \\ 0.84647 & 1.68525 & 1.73964 \\ 3.21803 & -3.25422 & -4.47055 \\ -2.75548 & -1.91487 & 2.05804 \\ -1.59837 & 0.84089 & -1.88979 \end{bmatrix} \quad LW^T = \begin{bmatrix} 431.680 & 465.639 \\ -0.43847 & -0.42425 \\ -129.134 & -137.925 \\ 0.76350 & -102.389 \\ -0.14871 & 0.00295 \\ 0.07436 & 0.02668 \\ -0.36683 & -0.37590 \\ -0.39675 & -0.37239 \\ -0.56186 & -0.63159 \\ 295.975 & 316.446 \\ -0.35951 & -0.51021 \\ -149.621 & -147.454 \\ -0.77523 & -0.51662 \\ 0.42429 & 0.46957 \\ -0.34559 & -0.35900 \\ -0.15489 & -0.01412 \\ 0.24867 & 0.25486 \\ 0.87009 & 117.698 \\ 0.65821 & 0.51646 \\ -279.617 & -310.858 \\ -0.72280 & -0.56382 \\ -0.60081 & 0.59206 \end{bmatrix} \quad B_1 = \begin{bmatrix} 6.10298 \\ 3.29456 \\ 3.83885 \\ -2.92241 \\ 3.60819 \\ 1.46528 \\ 0.11523 \\ 1.22986 \\ -0.69416 \\ -3.57305 \\ 2.03376 \\ -1.50434 \\ 1.22399 \\ 0.65199 \\ 0.77371 \\ -1.92857 \\ 0.58153 \\ 2.48658 \\ 3.54596 \\ 3.68079 \\ -3.59276 \\ -4.77956 \end{bmatrix} \quad B_2 = \begin{bmatrix} 0.76976 \\ 0.36829 \end{bmatrix}$$

Journal Pre-proofs

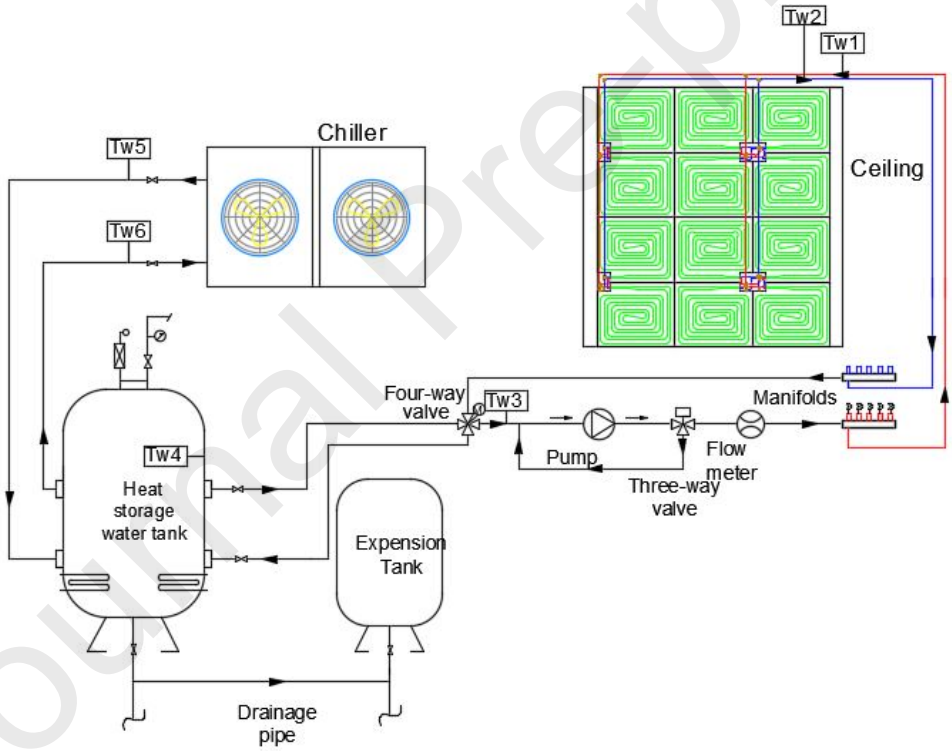
Table 8 Weight and bias matrix for heat transfer outputs

$$IW = \begin{bmatrix} 3.67709 & -0.80793 & -2.77018 \\ -0.99266 & -18.9885 & -2.10952 \\ 2.35401 & 0.76842 & -2.73194 \\ -1.47561 & -1.43803 & 3.29049 \\ -2.25803 & 3.11402 & -1.10820 \\ 3.48163 & -0.67698 & -0.92473 \\ -1.62023 & -2.63144 & 6.48576 \end{bmatrix} \quad LW^{T} = \begin{bmatrix} 0.58504 & -106.700 & -0.74759 \\ 223.592 & 0.44954 & 218.898 \\ 0.95163 & -204.296 & -0.79702 \\ 349.100 & 174.804 & 249.793 \\ -0.38718 & -289.934 & -235.146 \\ 0.21661 & 273.583 & 0.89587 \\ -416.979 & -132.739 & -296.970 \end{bmatrix} \quad B_1 = \begin{bmatrix} -2.51538 \\ 17.23321 \\ -0.32975 \\ 1.28429 \\ 0.66674 \\ 2.57296 \\ 3.72422 \end{bmatrix} \quad B_2 = \begin{bmatrix} 0.13042 \\ -2.13356 \\ -1.60562 \end{bmatrix}$$

Journal Pre-proofs



a)



b)

Fig. 1 General view of the test room (a) and hydraulic circuit of the test system (b)

Journal Pre-proofs

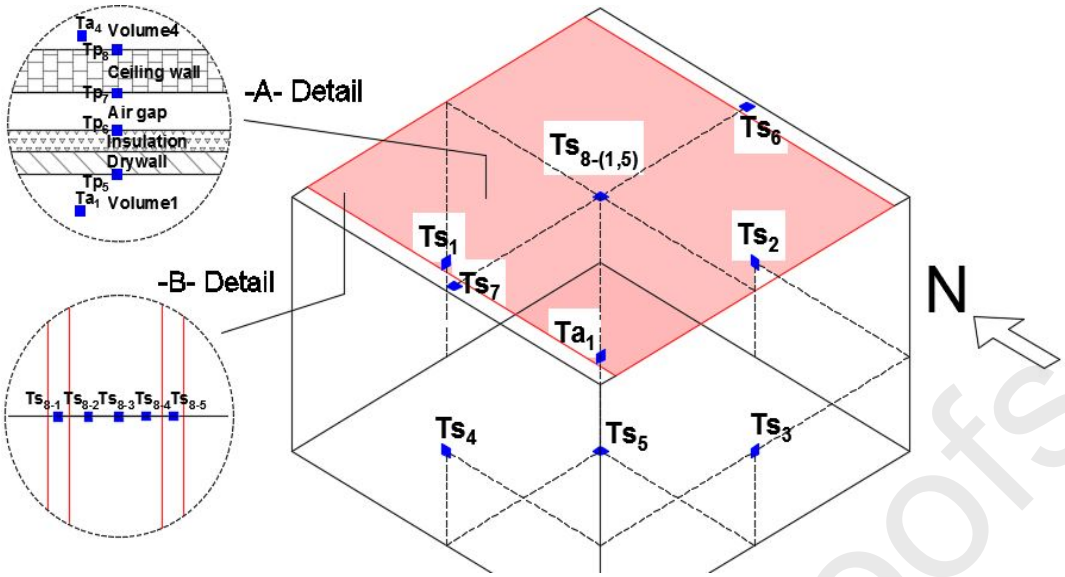


Fig. 2 Locations of the temperature sensors

Journal Pre-proofs

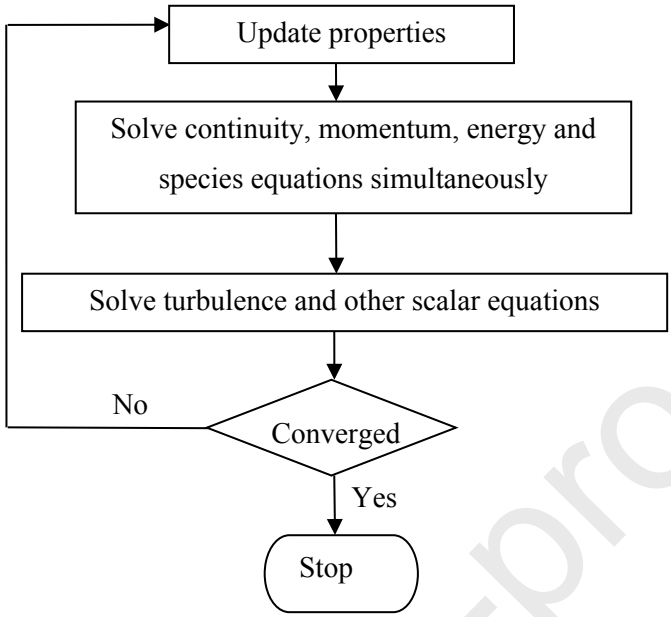


Fig. 3 The general steps pursued in each iteration to solve governing equations

Journal Pre-proofs

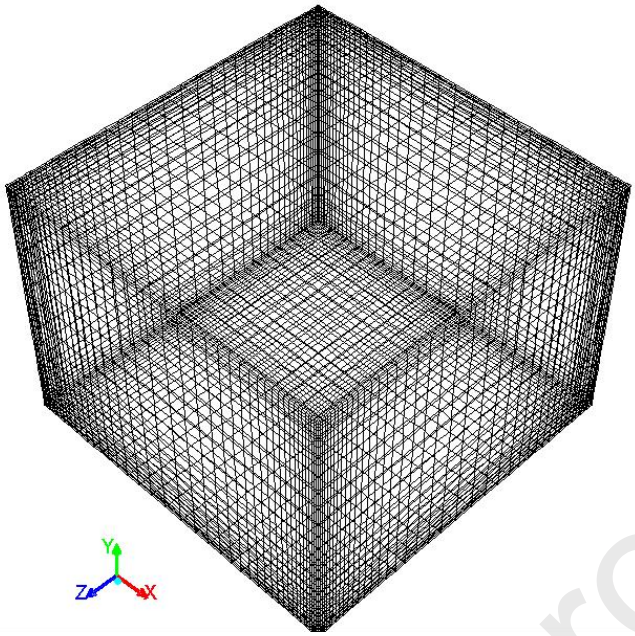


Fig. 4 Meshing of the numerically examined experimental chamber (LxHxW= 4x3x4 m)

Journal Pre-proofs

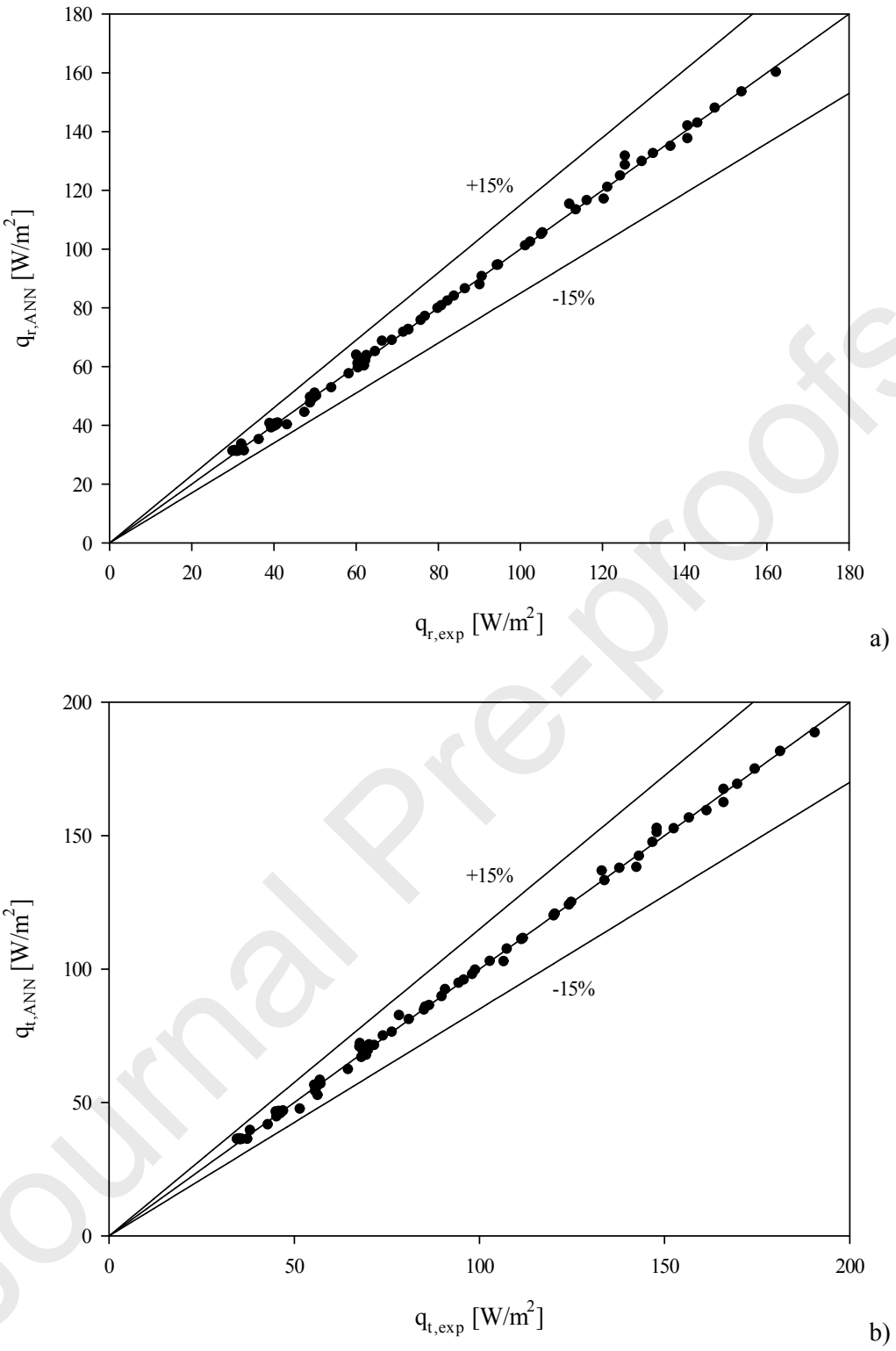


Fig. 5 Comparison of radiative heat flux data (a) and total heat flux data (b) obtained by experimental and ANN methods

Journal Pre-proofs

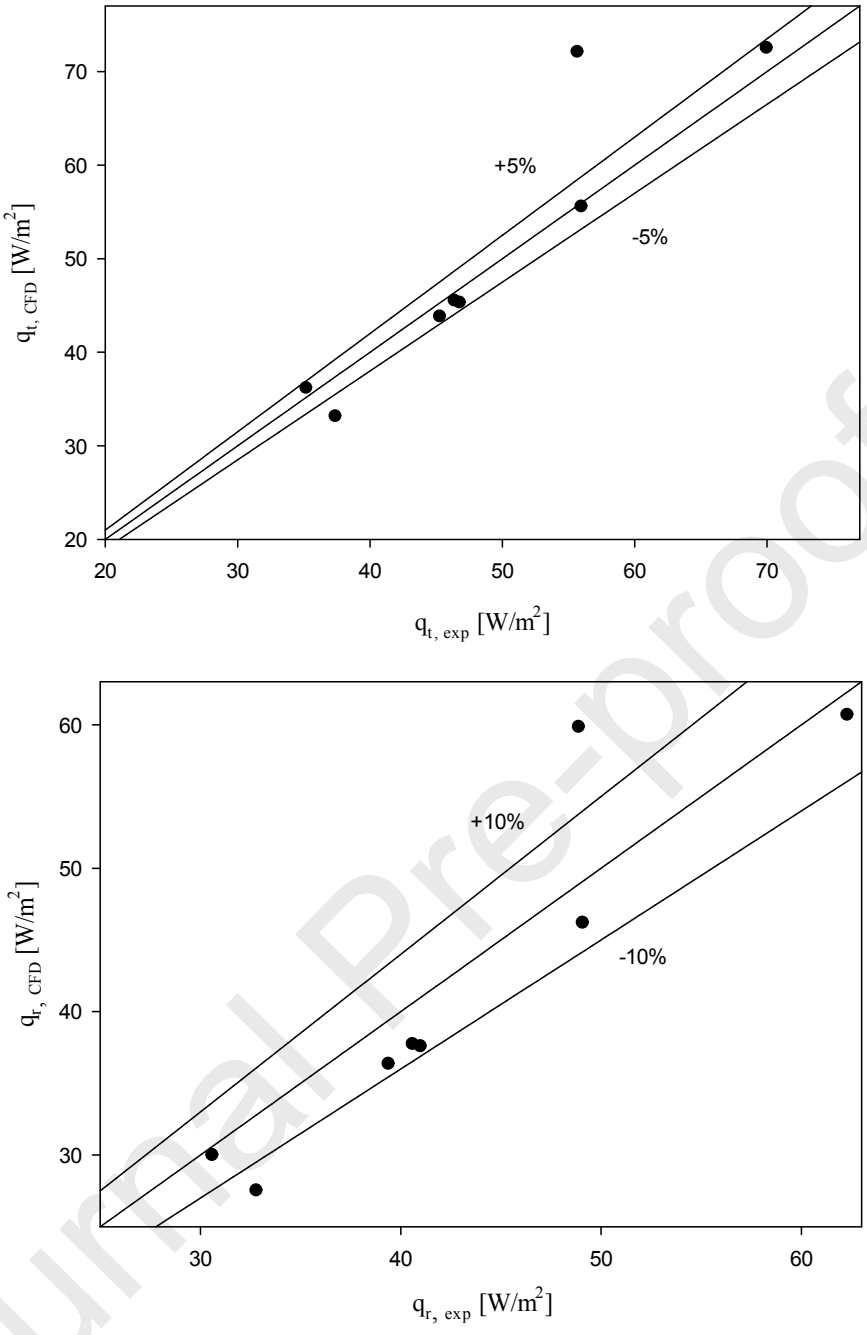


Fig. 6 Comparison of radiative heat flux data (a) and total heat flux data (b) obtained by experimental and CFD methods

Journal Pre-proofs

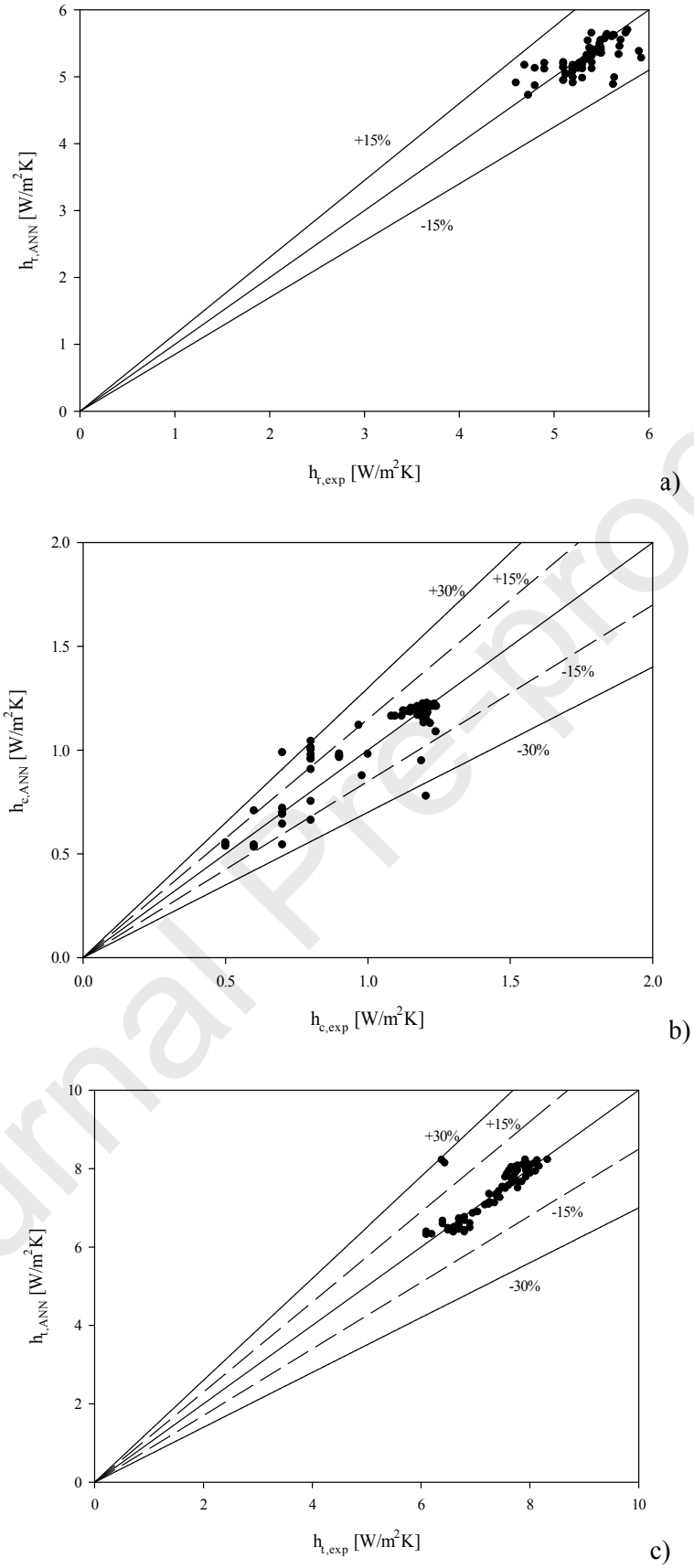


Fig. 7 Comparison of radiative heat transfer coefficient results (a), convective heat transfer coefficient results (b) and total heat transfer coefficient results (c) obtained by experimental and ANN methods

Journal Pre-proofs

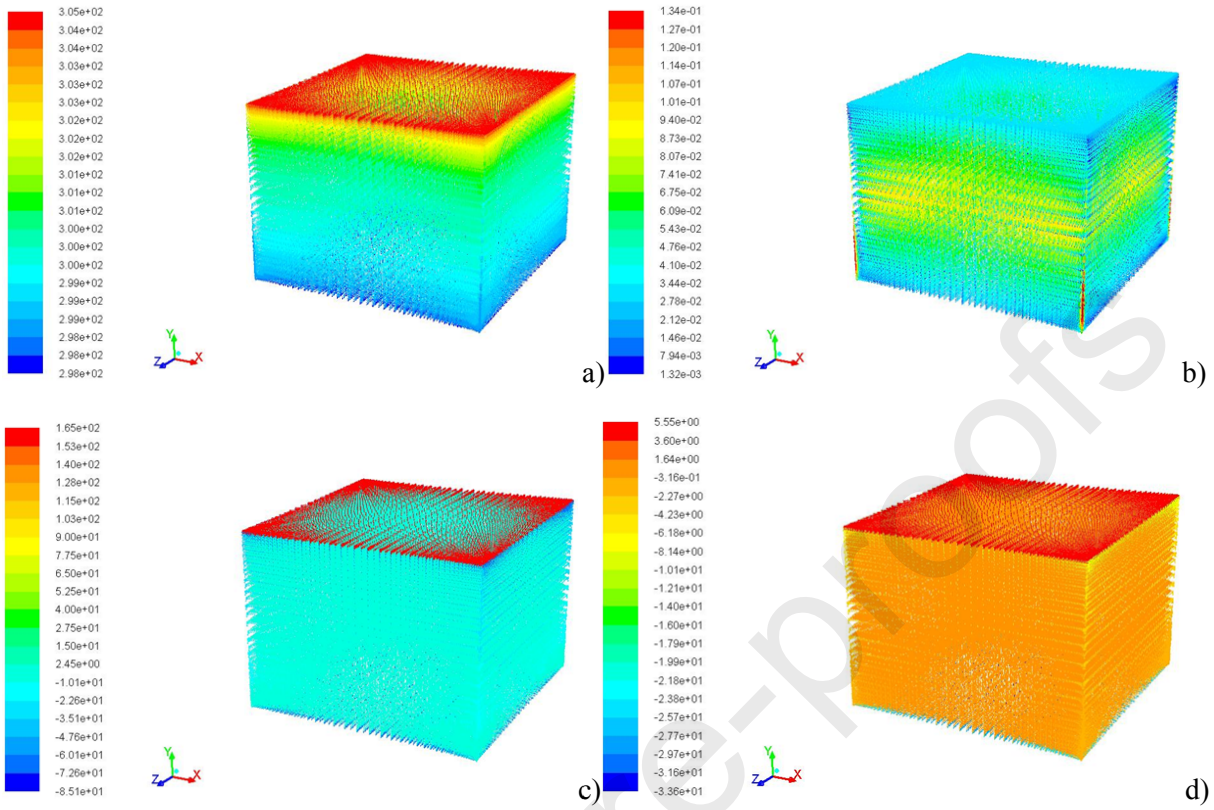


Fig. 8 Temperature contours and a number of vectors acquired by means of CFD software (a) temperature contour, (b) velocity vectors, (c) radiant heat flux vectors, and (d) surface heat transfer coefficient vectors

Journal Pre-proofs

Journal Pre-proofs

AUTHORSHIP STATEMENT

Manuscript title: A Comprehensive Approach to Analyze the Discrepancies in Heat Transfer Characteristics Pertaining to Radiant Ceiling Heating System

All persons who meet authorship criteria are listed as authors, and all authors certify that they have participated sufficiently in the work to take public responsibility for the content, including participation in the concept, design, analysis, writing, or revision of the manuscript. Furthermore, each author certifies that this material or similar material has not been and will not be submitted to or published in any other publication before its appearance in the Applied Thermal Engineering.

Authorship contributions

Category 1

Conception and design of study: O. Acikgoz, A.S. Dalkilic, S. Wongwises

acquisition of data: A. Koca, G. Çetin

analysis and/or interpretation of data: Y. Karakoyun, A. Çebi

Category 2

Drafting the manuscript: Y. Karakoyun, O. Acikgoz, A. Koca

revising the manuscript critically for important intellectual content: A.S. Dalkilic, O. Acikgoz, S. Wongwises

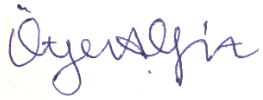
Category 3

Approval of the version of the manuscript to be published (the names of all authors must be listed): Yakup Karakoyun, Ozgen Acikgoz, Alican Çebi, Aliihsan Koca, Gürsel Çetin, Ahmet Selim Dalkilic, Somchai Wongwises

Acknowledgements

All persons who have made substantial contributions to the work reported in the manuscript (e.g., technical help, writing and editing assistance, general support), but who do not meet the criteria for authorship, are named in the Acknowledgements and have given us their written permission to be named. If we have not included an Acknowledgements, then that indicates that we have not received substantial contributions from non-authors.

This statement is signed by corresponding author on behalf of others authors:



Assoc. Prof. Dr. Ozgen Acikgoz

Journal Pre-proofs

Conflict of interest

On behalf of all authors, the corresponding author states that there is no conflict of interest.

Dr. Ozgen Acikgoz

Yildiz Technical University, Department of Mechanical Engineering
Thermodynamics and Heat Transfer Division
Besiktas Istanbul Turkey
Tel: 90 212 383 29 14
Fax: 90 212 261 66 59
e-mail: oacikgoz@yildiz.edu.tr

Journal Pre-proofs